Benefits of Variable Speed Pumped Storage Units in Mixed Islanded Power Network during Transient Operation

C. Nicolet
Power Vision Engineering sàrl
1 ch. Champs-Courbes
1024 Ecublens
Switzerland

Y. Pannatier
Laboratory of Electrical Machines
EPFL
1015 Lausanne
Switzerland

B. Kawkabani
Laboratory of Electrical Machines
EPFL
1015 Lausanne
Switzerland

A. Schwery
ALSTOM (Switzerland) Ltd
Zentralstrasse 40
5242 Birr
Switzerland

F. Avellan
Laboratory for Hydraulic Machines
33 bis av. Cour
EPFL
1007 Lausanne
Switzerland

J.-J. Simond
Laboratory of Electrical Machines
EPFL
1015 Lausanne,
Switzerland

Abstract

This paper presents the modeling, simulation and analysis of the dynamic behavior of a mixed islanded power network of 1'750 MW comprising 1'300 MW of classical thermal power plant, 200 MW of wind power and 250 MW of hydropower. First, the modeling of each power plant is fully described. The model of the thermal power plants includes constant pressure steam tank, a high-pressure steam turbine, a re-heater, and 2 low pressure steam turbines, the rotating inertias, and a 1'400 MVA turbo-generator with proportional power controller and a voltage regulator. The 200 MW wind farm is modeled through an equivalent machine approach of 100 wind turbines of 2MW. The wind farm model comprises a stochastic model of wind evolution with wind gust, a power coefficient based model of wind turbine with a-priori controller and a synchronous generator with voltage regulator. Finally, the 250 MW pumped storage power plant model comprises the upstream reservoir, a 1950 meters gallery, a surge tank, the 885 meters long penstock feeding a variable speed unit pump-turbine connected to the downstream tank through a 250 meters long tailrace water tunnel. The variable speed unit comprises a Doubly Fed Asynchronous Motor-Generator equipped with a back-to-back VSI (Voltage Source Inverter) cascade. The 3 power plants are connected to a passive consumer load via a 500 KV electrical line network. Then, the capability of the pumped storage plant to stabilize the islanded power network is investigated through the time domain simulation of the dynamic behavior of the entire mixed power network using the software SIMSEN. Three different scenarios are considered: (i) partial load rejection enabled by flywheel effect in generating mode, (ii) load acceptance step enabled by flywheel effect in pumping mode, (iii) wind power fluctuations are compensated by pump power adjustment through rotational speed variation. The simulation results obtained with variable speed unit are compared with simulation results obtained with same pumped storage power plant but equipped with three-machine-type unit with fixed speed synchronous generator. Safe and stable operation for the 3 above mentioned scenarios are presented and comparison between fixed speed and variable speed results are discussed.

1. Introduction

As wind energy is highly volatile energy source, islanded power networks featuring high level of wind power penetration are subjected to undesired perturbation jeopardizing the power network stability [25]. Consequently, pumped storage plants can significantly improve the stability of mixed islanded power network due to their production flexibility. The high dynamic performances of such pumped storage plants are of highest interest for improving stability of mixed islanded power network.

Variable speed pump-turbine units have become nowadays major partner to increase stability of electrical power networks due to their high level of operating flexibility, [12], [19], [20]. Indeed, variable speed pump-turbine units offer several advantages for both pumping and generating modes such as: (i) possibility of active power control in pumping mode, (ii) efficiency increase and wide range of operation in generating mode especially under partial load, (iii) network stability improvement by reactive power control and (iv) network stability improvement by instantaneous active power injection in the grid (flywheel effect). Extended operating range in pump mode and higher efficiency in turbine mode achievable with variable speed units are illustrated in Figure 1.

Three-machine-type units, with turbine, generator, fluid coupling clutch and pump, offer also numbers of operation advantages despite a higher investment cost compared to variable speed pump-turbine. The operation advantages of the 3-machine-type units are the following [4], [15]: (i) increased efficiency in pump and turbine modes, (ii) high operational flexibility due to rapid change of operation mode from pump to turbine and vice-

versa, (iii) easy and short time start-up in pump mode, (iv) adjustable pump power in hydraulic short-circuit operation, (v) efficient condenser modes.

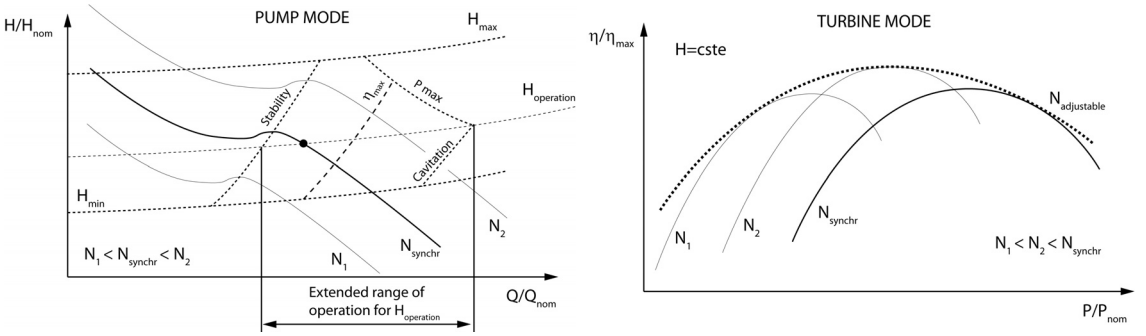

Figure 1 Advantages of variable speed machines compared to fixed speed machines for pump (left) and turbine (right) mode of operation.

This paper presents the modeling, numerical simulations and analysis of the stability of a mixed islanded power network of 1'750 MW comprising 1'300 MW of classical thermal power plant, 200 MW of wind power and 250 MW of hydropower. The 3 power plants are connected to a passive consumer load via a 500 KV electrical line network as presented in Figure 2. For the hydraulic power plant, two different technical solutions are considered:

- reversible pump-turbine with variable speed unit comprising a Doubly Fed Asynchronous Motor-Generator (DFIG) equipped with a back-to-back VSI (Voltage Source Inverter) cascade;
- three-machine-type unit with fixed speed synchronous motor-generator.

First, the modeling of each power plant is fully described. Then, the capability of the pumped storage plant to stabilize the islanded power network is investigated through the time domain simulation of the dynamic behavior of the entire mixed power network using the software SIMSEN. Three different scenarios are considered: (i) partial load rejection in turbine mode, (ii) load acceptance step in pumping mode, (iii) wind power fluctuations compensation in pumping mode. The simulation results obtained with variable speed unit are compared with simulation results obtained with fixed speed three-machine-type unit. Safe and stable operation for the 3 above mentioned scenarios are presented and comparison between fixed speed and variable speed results are discussed.

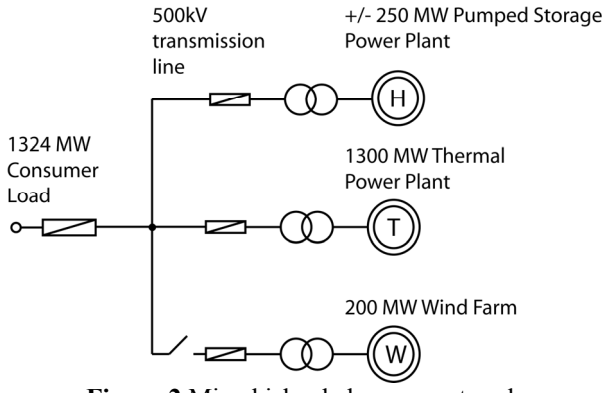

Figure 2 Mixed islanded power network.

2. Modeling of the Hydraulic Machinery and Systems

By assuming uniform pressure and velocity distributions in the cross section and neglecting the convective terms, the one-dimensional momentum and continuity balances for an elementary pipe filled with water of length *dx*, cross section *A* and wave speed *a*, see Figure 3, yields to the following set of hyperbolic partial differential equations [26]:

$$\begin{cases} \dfrac{\partial h}{\partial t} + \dfrac{a^2}{gA} \cdot \dfrac{\partial Q}{\partial x} = 0 \\ \dfrac{\partial h}{\partial x} + \dfrac{1}{gA} \cdot \dfrac{\partial Q}{\partial t} + \dfrac{\lambda |Q|}{2gDA^2} \cdot Q = 0 \end{cases} \tag{1}$$

The system (1) is solved using the Finite Difference Method with a 1st order center scheme discretization in space and a scheme of Lax for the discharge variable. This approach leads to a system of ordinary differential equations that can be represented as a T-shaped equivalent scheme [10], [17], [23] as presented in Figure 4. The RLC parameters of this equivalent scheme are given by:

$$R = \frac{\lambda \cdot |\overline{Q}| \cdot dx}{2 \cdot g \cdot D \cdot A^2} \qquad L = \frac{dx}{g \cdot A} \qquad C = \frac{g \cdot A \cdot dx}{a^2} \tag{2}$$

Where λ is the local loss coefficient. The hydraulic resistance R, the hydraulic inductance L, and the hydraulic capacitance C correspond respectively to energy losses, inertia and storage effects.

The model of a pipe of length *L* is made of a series of n_b elements based on the equivalent scheme of Figure 4. The system of equations relative to this model is set-up using Kirchoff laws. The model of the pipe, as well as the model of valve, surge tank, Francis turbine, etc, is implemented in the EPFL software SIMSEN, developed for the simulation of the dynamic behavior of hydroelectric power plants, [13], [18]. The time domain integration of the full system is achieved in SIMSEN by a Runge-Kutta 4th order procedure.

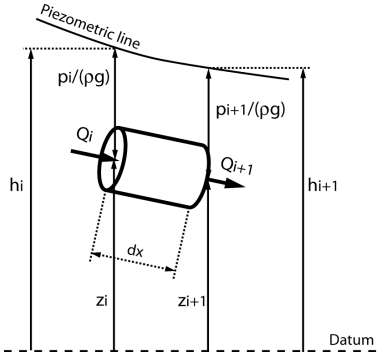

Figure 3 Elementary hydraulic pipe of length dx.

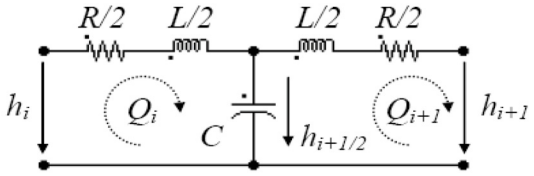

Figure 4 Equivalent circuit of an elementary pipe of length dx.

As presented in Table 7 of Appendix 2, the modeling approach based on equivalent schemes of hydraulic components is extended to all the standard hydraulic components such as valve, surge tanks, air vessels, cavitation development, Francis pump-turbines, Pelton turbines, Kaplan turbines, pump, etc, see [13].

3. Hydraulic Power Plant Model

The layout of the hydraulic power plant is presented in Figure 5. The power plant is made of an upstream reservoir, a 1'950 meters long gallery, a 885 meters long penstock connected to a hydroelectric power house of +/-250 MW and connected to the downstream reservoir by a tailrace water tunnel of 250 meters long. For the power house, two different solutions are compared:

- three-machine-type arrangement with fixed speed synchronous generator of 280MVA;
- reversible pump-turbine with variable speed (VarSpeed) doubly fed induction generator (DFIG) of 280MVA.

Table 1 gives the main characteristics of the pumped-storage power plant used for both fixed and variable speed solutions. The models of the two solutions are presented in the two sub-chapters below. For both models, the hydraulic machines are modeled using their 4 quadrants characteristics. The model of the piping system accounts for detailed water-hammer and mass oscillation phenomena, [13].

Table 1 Pumped-storage power plant characteristics.

Pump-Turbine / Pump / Turbine	**Generator**
P_R=250 MW	Rated apparent power: 280 MVA
N_R=500 rpm	Rated phase to phase voltage: 17.5kV
Q_R=55 m^3/s	Frequency: 50 Hz
H_R=510 m	Number of pairs of poles: 6
ν=0.22	Stator windings: Y
$J_{pump\text{-}turbine}$=1.05*10^5 kgm^2	J_{rotor}=8.1*10^5 kgm^2

3.1. Fixed Speed Pumped Storage Power Plant Model with Synchronous Generator

The 3 machine-type arrangement model considered in this paper is presented in Figure 5. This model is composed of a Francis turbine of 250 MW, the synchronous generator of 280 MVA, a pump of 250 MW and a clutch between the generator and the pump. The clutch characteristic is taken from [2]. The turbine is equipped with a PID turbine speed governor and the generator is controlled by an ABB Unitrol voltage regulator. The model of the generator is based on 1 equivalent rotor circuit in the direct-axis and 1 equivalent rotor circuit in the quadrature-axis allowing taking into account a sub-transient behavior, see [5].

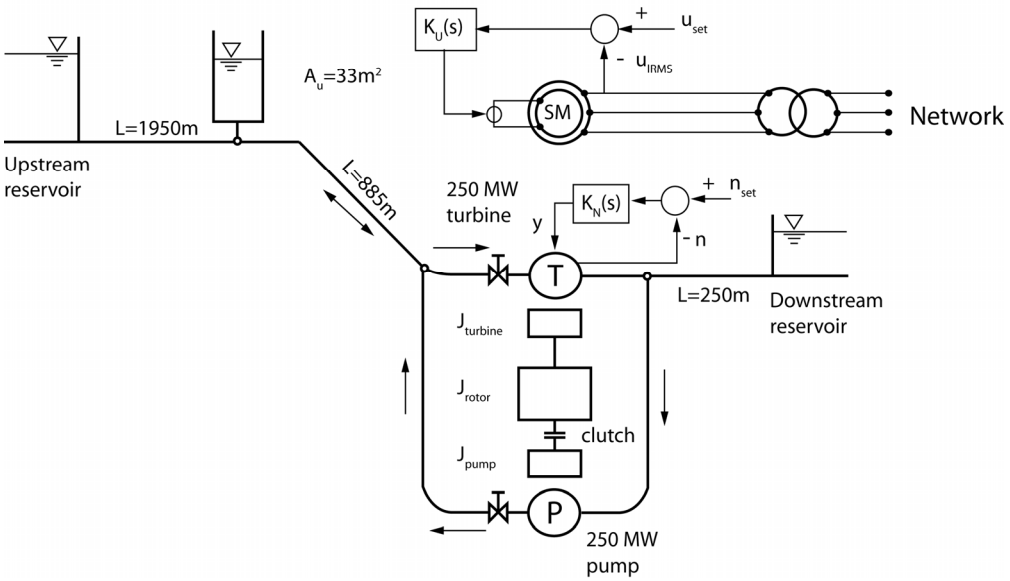

Figure 5 Pumped storage power plant model with fixed speed and 3 machine-type arrangement.

3.2. Variable Speed Pumped Storage Power Plant Model with Doubly Fed Induction Generator

The variable speed unit model considered in this investigation is presented in Figure 6.

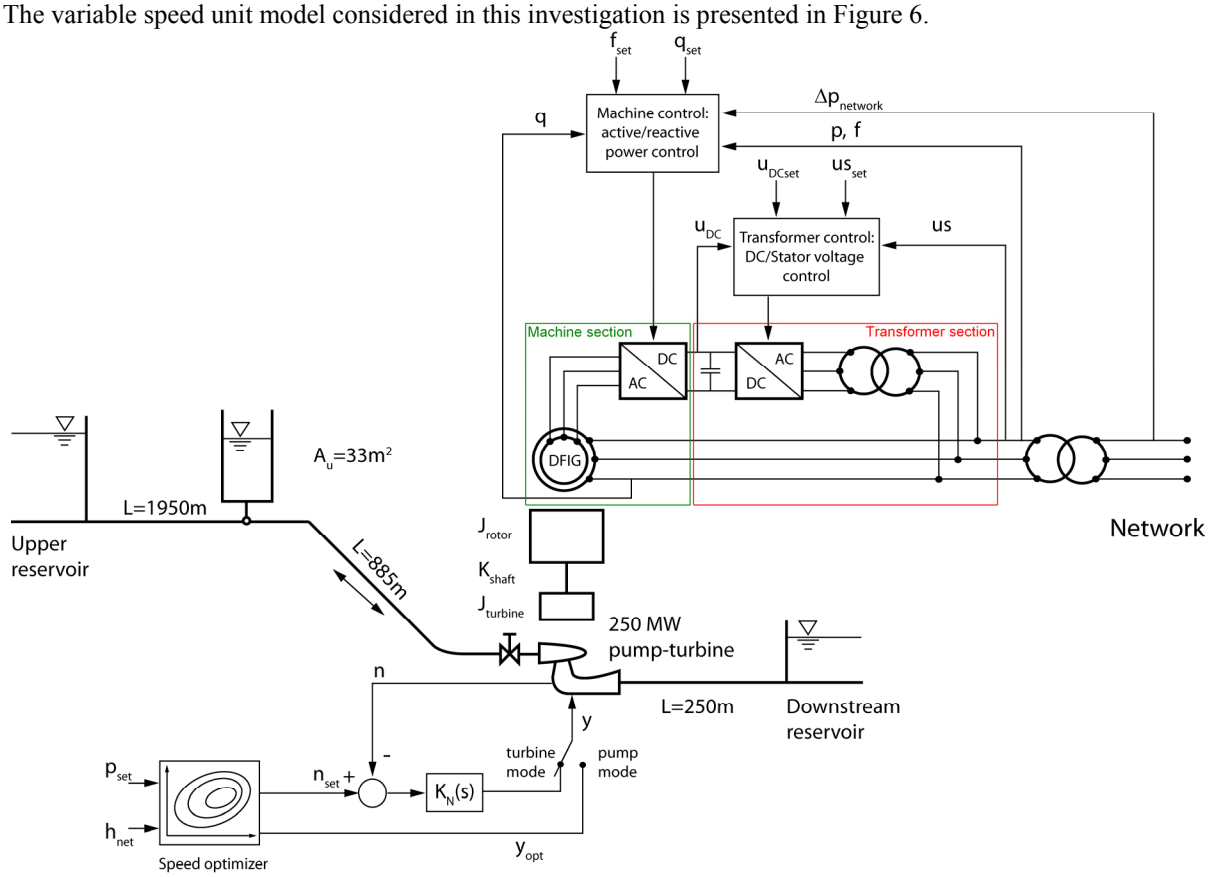

Figure 6 Pumped storage power plant model with variable speed pump-turbine.

The same hydraulic layout is considered except for the hydraulic machine which is replaced by a reversible pump-turbine of 250MW. The pump-turbine is driven using a speed optimizer which defines optimum speed in turbine mode and optimum guide vane opening in pump mode according to power and net head operating conditions, see [7], [11], [16]. The electrical system comprises a doubly fed induction motor-generator with 2 level VSI (Voltage Source Inverter) cascade in the rotor side. The model of the induction machine is based on classical d, q Park equations expressed in a, b, c quantities.

This electrical system can be divided into two sections, a transformer section and a machine section, see Figure 6. The transformer section operates as a Static Var Compensator (SVC), its main role being to exchange reactive power with the grid. The reactive power and the capacitors voltage are controlled by acting on the transformer primary side currents through the right-side converter. The main role of the machine section is to control the active power of the machine. The active power and the stator reactive power of the machine are controlled by acting on the rotor currents through the left-side converter. The control structure of the transformer and machine sections are presented in Figure 7.

As this hydropower plant is operating in islanded power network, a special care has been paid to set up the active power control structure in order to have fast response of the variable speed unit to network disturbances. Therefore, the active power set point of the DFIG accounts for network frequency deviations but also for power variation in the power network $\Delta p_{network}$, see [24]. This power variation is calculated as:

$$\Delta p_{network} = p_{load} - p_{set\_therm} - p_{wind} \tag{3}$$

This approach assumes that it is possible to measure the output power of the wind farm, the thermal power plant set point and the power consumption of the load. This approach is particularly relevant for small power networks with small number of producers and consumers where the hydropower plant has a significant power output compared to the total power.

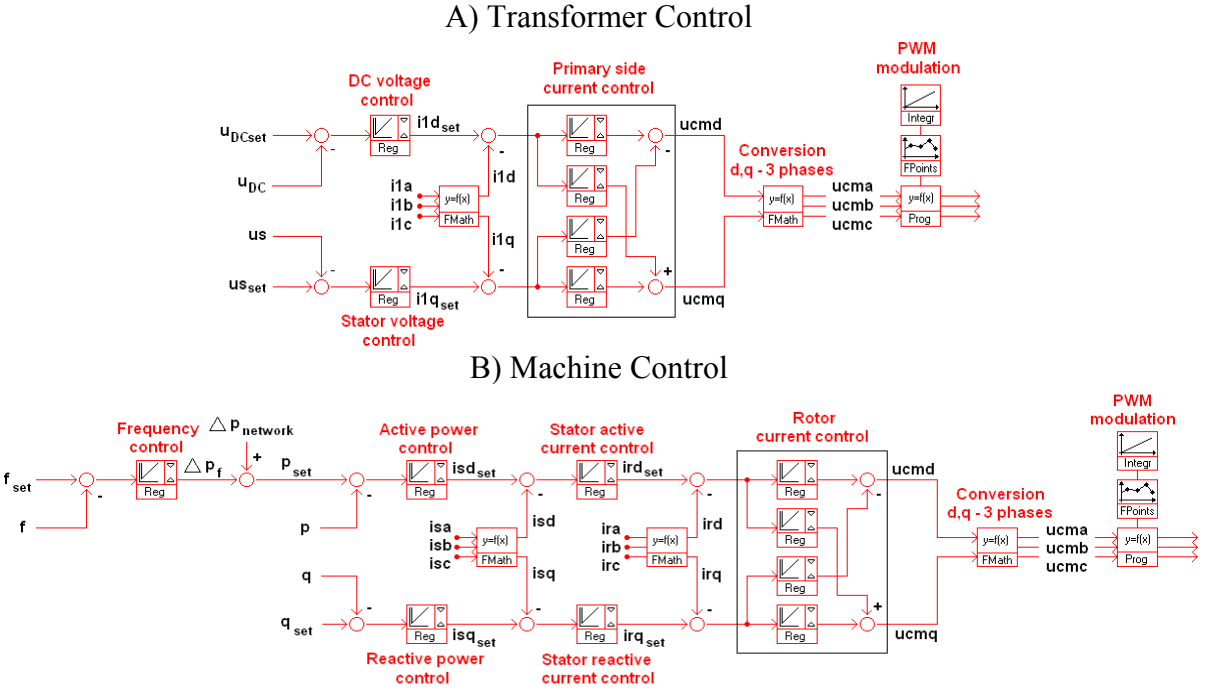

Figure 7 Transformer and machine control structures.

4. Thermal Power Plant Model

The model of the 1.3 GW thermal power plant is based on steam flux and takes into account a constant pressure steam vessel, a regulating valve, a high pressure steam turbine, a steam transit through a re-heater and two low pressure steam turbines as presented in Figure 8. The model is based on valve and torque characteristics deduced from [3], on first order transfer functions for the turbine dynamics with τ_{HP}, τ_{LP} time constants, a re-heater modeled by a time delay b, and on a proportional regulator of constant Kp. The shaft line comprises 4 rotating inertias connected by 3 shafts with given stiffness and damping. And finally a turbo generator with 2 pairs of poles is also included in the model with the ABB Unitrol voltage regulator. The model of the generator is based

on 2 equivalent rotor circuits in the direct-axis and 1 equivalent rotor circuit in the quadrature-axis considering saturation, leakage and damping effects of windings, allowing taking into account a sub-sub-transient behavior, see [5]. The parameters of the model are given in Table 2 and details of the model can be found in [14].

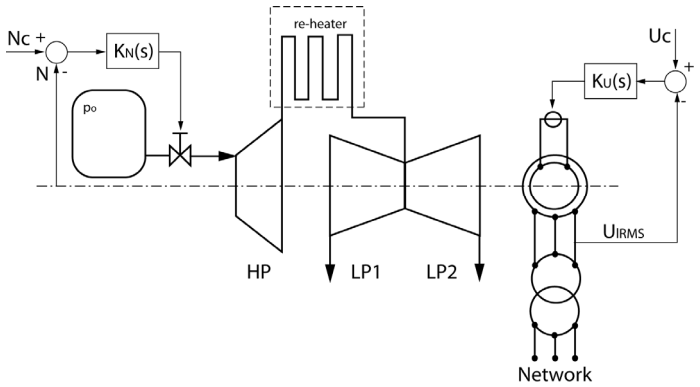

Figure 8 Thermal power plant model.

Table 2 Thermal power plant characteristics.

Steam turbines model	**Mechanical masses inertias**	**Mechanical shaft stiffness and damping**	**Generator**
τ_{HP} = 0.5 s τ_{LP} = 12 s b = 4 s Kp = 25	$J_{HP} = 1.867*10^4$ Kgm^2 $J_{LP1} = 1.907*10^5$ Kgm^2 $J_{LP2} = 2.136*10^5$ Kgm^2 $J_{GEN} = 5.223*10^4$ Kgm^2	$K_1 = 3.614*10^8$ Nm/rd $K_2 = 8.206*10^8$ Nm/rd $K_3 = 4.116*10^8$ Nm/rd $\mu_1 = 6.719*10^3$ Nms/rd $\mu_2 = 7.06*10^3$ Nms/rd $\mu_3 = 7.06*10^3$ Nms/rd	Rated apparent power: 1400 MVA Rated phase to phase voltage: 28.5kV Frequency: 50 Hz Number of pairs of poles: 2 Stator windings: Y

5. Wind Farm Model

5.1. Wind Turbine Model

The model of a 2 MW wind turbine is presented in Figure 9. It includes a model of the turbulent wind, the turbine with adjustable blade pitch angle θ and inertia $J_{turbine}$, the shaft stiffness k_{shaft}, the gear box, the synchronous generator of 2 MVA with voltage regulator and the transformer. The characteristics of the wind turbine model are given in Table 3. The model of the generator is based on 1 equivalent rotor circuit in the direct-axis and 1 equivalent rotor circuit in the quadrature-axis allowing taking into account a sub-transient behavior, see [5].

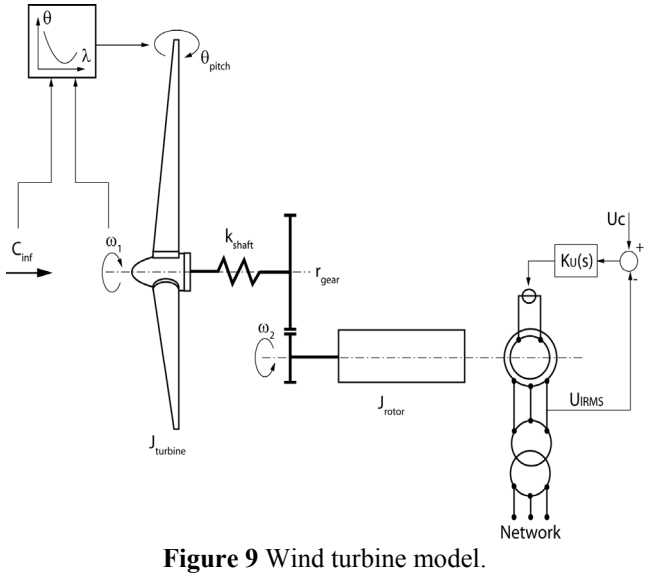

Figure 9 Wind turbine model.

Table 3 Wind turbine characteristics.

Operating datas	Wind turbine	Mechanical system	Generator
Cut-in wind velocity: 3.5 m/s Cut-out wind velocity: 20 m/s Rated wind velocity: 13 m/s	Number of blades: 3 Diameter: D=75 m Rotational Speed: n1=24.75 rpm	r_{gear}= 3.032 k_{shaft} = 2.2*10^8 Nm/rd $J_{turbine}$= 3.15*10^6 kgm^2 J_{rotor}= 6.48*10^4 kgm^2	Rated apparent power: 2 MVA Rated phase to phase voltage: 400 V Frequency: 50 Hz Number of pairs of poles: 40 Stator windings: Y

The turbulent wind model is composed of a wind mean value and a wind gust, as suggested by Slootweg *et al.* [21]. The turbulent gust is modeled by a Pseudo-Random-Binary-Sequence, PRBS, obtained by a shift register method, see [6]. The mechanical power transmitted by the fluid to the wind turbine can be expressed as:

$$P = \frac{1}{2}\rho \cdot Aref \cdot Cp \cdot C_{\inf}^3 \qquad (4)$$

Where A_{ref} is the swept area and C_p is the power coefficient and ρ is the air density. Heier [8] provides an empiric approximation of the wind turbine power coefficient C_p as function of the tip speed ratio λ is defined as:

$$\lambda = \frac{U_t}{C_{\inf}} = \frac{D_{ref} \cdot \omega_1}{2 \cdot C_{\inf}} \qquad (5)$$

Where U_t is the blade tip velocity, C_{inf} is the wind velocity and ω_1 is the wind turbine rotating pulsation. Figure 10 left presents the power coefficient C_p of a wind turbine as function of the tip speed ratio λ and of the blade pitch angle θ obtained according to [8].

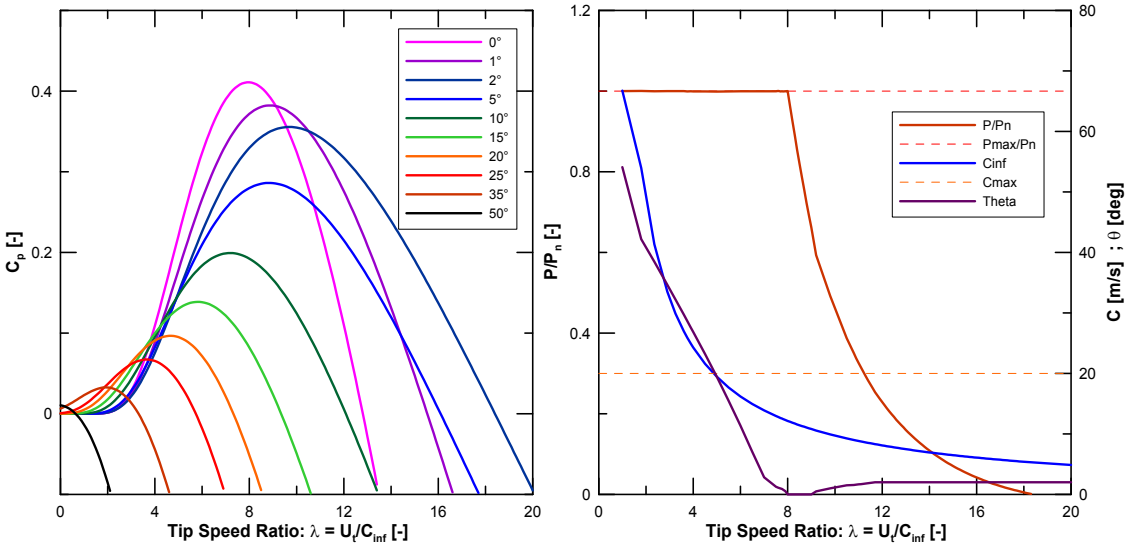

Figure 10 Wind turbine characteristic according to equation (4) (left) and wind turbine power, pitch angle and wind velocity and related limits as function of the tip speed ratio (right).

Then, the wind turbine output power is calculated from Figure 10 left, as function of the tip speed ratio as presented in Figure 10 right, see also [22]. The blade pitch angle given as function of the tip speed ratio is also represented in Figure 10 right. For tip speed ratio above 8, the pitch angle is selected to provide the highest power coefficient while below 8 it is selected to generate the 2 MW output power limit. The blade pitch angle θ is driven by a look-up table as function of the tip speed ratio λ as represented in Figure 10 right.

5.2. Aggregated Wind Farm model

For power grid stability purposes, it is possible to use an aggregated wind farm model, consisting of one wind turbine equivalent to *n* single wind turbines as presented in Figure 11, see [1]. Then according to the energy conservation and in order to keep the same torsional mode eigenfrequency, the active power P_n, rotating inertias *J*, the shaft stiffness k_{shaft} and the swept area A_{ref} are multiplied by the number of wind turbines *n*. The parameters of the synchronous generator being given in per unit, they are kept constant. For the present study, only one equivalent machine can be used as no electrical faults are considered [1].

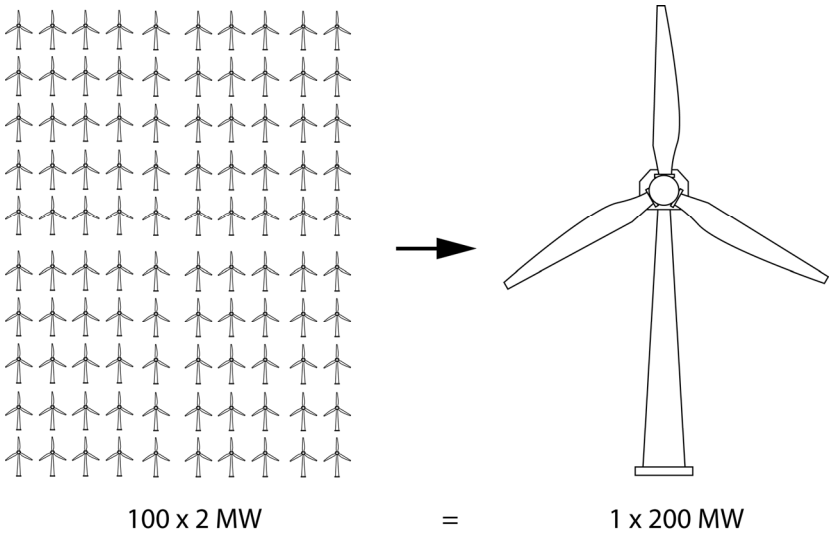

Figure 11 Wind turbine farm of 100 x 2 MW modeled as an equivalent wind turbine of 200 MW.

6. Mixed Islanded Power Network Model

Figure 12 presents the full SIMSEN model of the mixed islanded power network of Figure 2 based on the hydraulic, thermal and wind power plant models described above for the variable speed pump-turbine solution. The model also includes the 500 kV transmission lines and the passive consumer load. The SIMSEN model of the 3 machine-type solution can be found in [15].

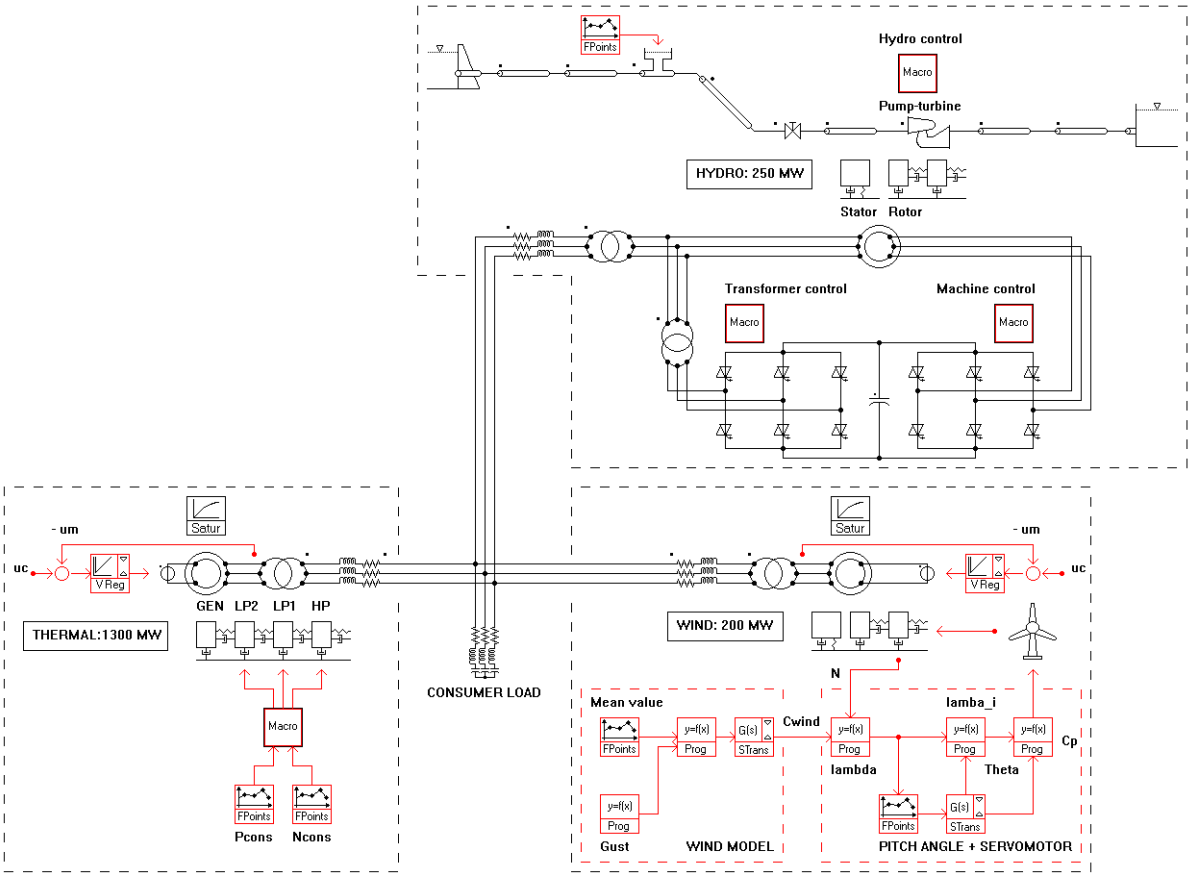

Figure 12 Mixed Islanded Power Network SIMSEN model**.**

7. Transient Behavior of Mixed Islanded Power Network

Three different cases studies are considered for the analysis of the dynamic behavior of the mixed islanded power network of Figure 12:

- load rejection in turbine mode,
- load acceptance in pumping mode,
- wind power fluctuations compensation by pump power adjustment.

The scenarios and simulation results related to the three cases studies stated above are described in the following subchapters. For simplicity, the pump-turbine speed optimizer of the variable speed solution has not been taken into consideration for these simulations. This only modifies initial and final steady-state operating rotational speed but does not affect transient behavior of the variable speed unit.

7.1. Partial load rejection in Turbine Mode of Operation

The first case study consists of a load rejection of 40MW simulated by reducing the consumer load instantaneously at the time t=10s. The initial conditions of the power flow of the islanded power network are summarized in Table 4. The three power plants are in generation operating conditions close to rated output power while the consumer load is consuming 1'726.1MW. The difference between the production and consumption corresponds to the energy losses in transmission lines and transformers.

Table 4 Initial power flow.

Element	Active power P [MW]	Power flow
Hydropower Plant	-244.7	Production
Thermal Power Plant	-1297.2	Production
Wind Farm	-189.2	Production
Consumer Load	+1726.1	Consumption

Figure 13 presents the simulation results obtained for both the variable speed and the fixed speed solutions. It can be seen that the variable speed machine is reducing almost instantaneously the generator output power and compensates the load rejection in less than 0.3s while the fixed speed unit takes about 150s to reduce its power output. The very fast response of the variable speed unit is enabled by the flywheel effect visible on the pump-turbine parameters evolution. Indeed, the fast variation of the generator output power induces a rotational speed increase and the extra pump-turbine output power is stored into kinetic energy of the rotating inertias [12]. This speed change is not problematic as the generator is a variable speed machine. Then the turbine speed governor changes the guide vane opening in order to recover the rotational speed set point. The head variation resulting from the pump-turbine transient is of about 3% of the rated head and is thus fully compatible with the penstock and tailrace water tunnel safety.

Regarding the simulation results obtained with the fixed speed solution, one may notice that the first seconds after the load rejection, the main contribution to the power network stability is provided by the thermal power plant enabled by the steam pressure tank reserves. However, if thermal power plant can provide power output variation during the first seconds, the output power set point of such power plant cannot be adapted very fast as it is restricted by the thermal power generation process controllability. Therefore, this is the hydropower plant which reduces its output power through the turbine speed governor action on the guide vane opening.

Figure 14 presents the comparison between the power network frequency obtained with variable speed and fixed speed solutions on the left and of the consumer load voltage on the right. It can be noticed that the frequency deviation in the case of the variable speed solution is lower than 0.05% while the frequency deviation reaches 0.55% in the case of the fixed speed. The comparison of the consumer load voltage shows large reduction of the voltage peak resulting from the load rejection.

However, one has also to notice that both the output power and the stator voltage provided by the variable speed machine features large content of harmonics. These harmonics can be considerably reduced by using a 3 level VSI instead of a 2 level VSI as it is shown in Appendix 1.

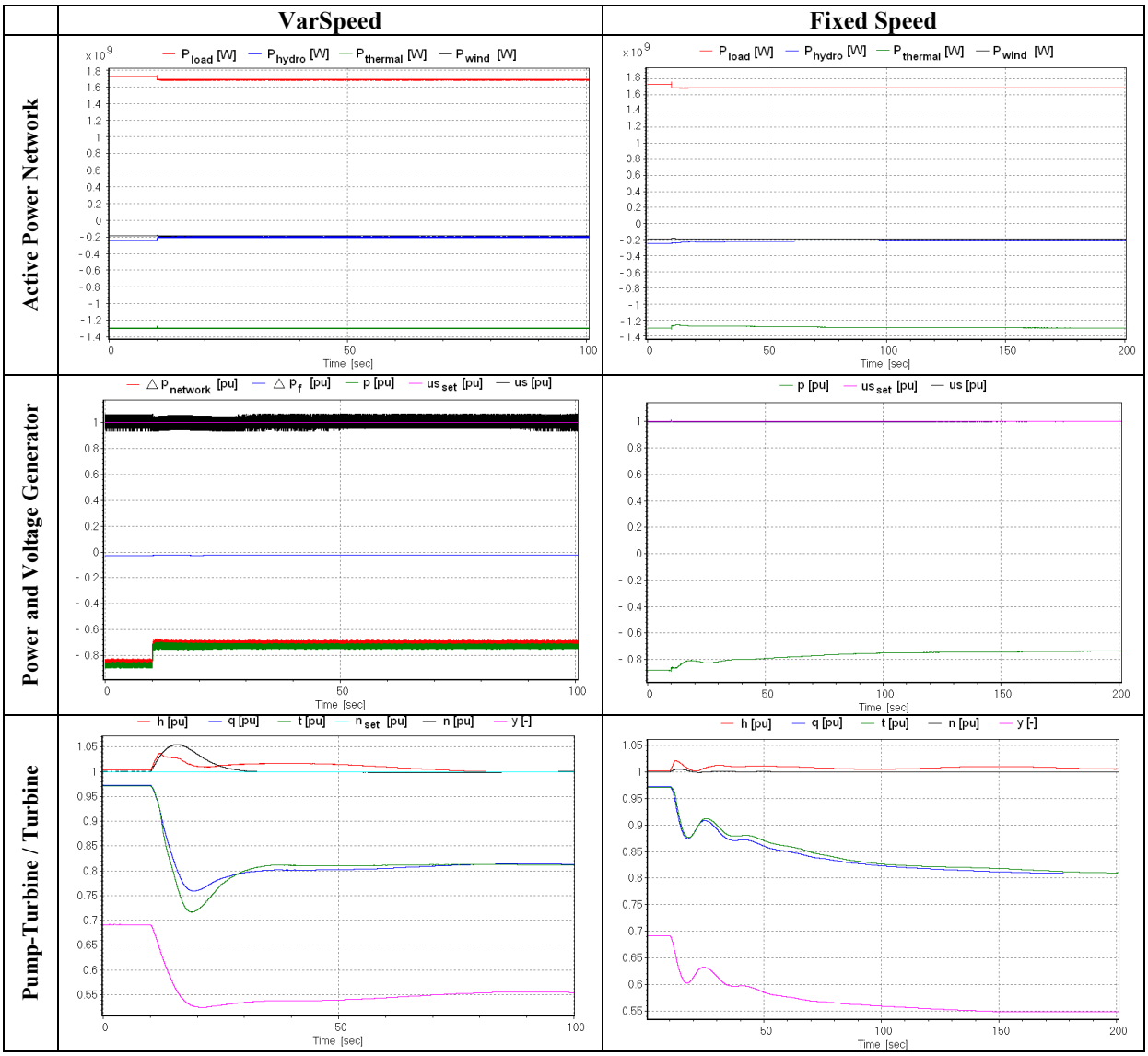

Figure 13 Comparison of the simulation results for both variable and fixed speed solutions for load rejection in turbine mode operation.

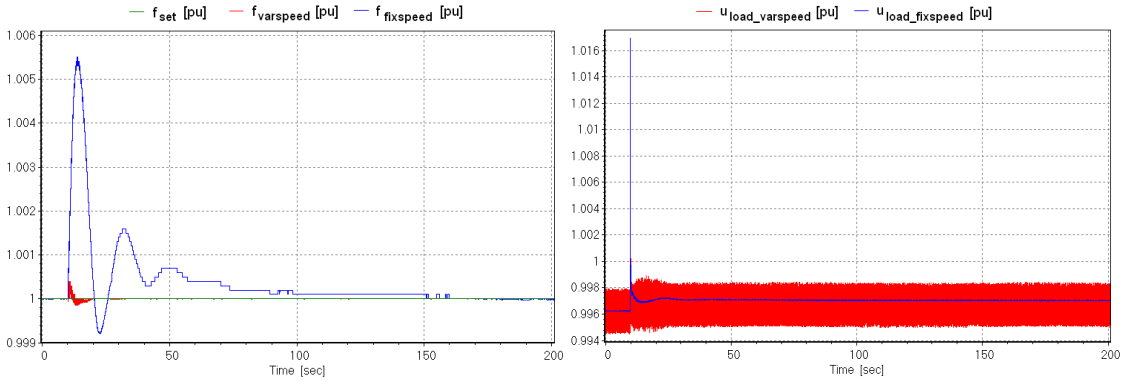

Figure 14 Comparison of the simulation results of the power network frequency (left) and voltage of the load (right) for both variable and fixed speed solutions for load rejection in turbine mode operation.

7.2. Load Acceptance Step in Pump Mode of Operation

The second case study consists of a load acceptance of 40MW simulated by increasing the consumer load instantaneously at the time t=10s. The initial conditions of the power flow of the islanded power network are summarized in Table 5. The thermal and wind farm power plants are in generation operating conditions close to rated output power while the hydraulic power plant is consuming extra wind power output by pump operation. The consumer load is consuming 1'232.4MW. Figure 15 presents the simulation results obtained for both the variable speed and the fixed speed solutions.

Table 5 Initial power flow.

Element	Active power P [MW]	Power flow
Hydropower Plant	+249.1	Consumption
Thermal Power Plant	-1297.2	Production
Wind Farm	-189.2	Production
Consumer Load	+1232.4	Consumption

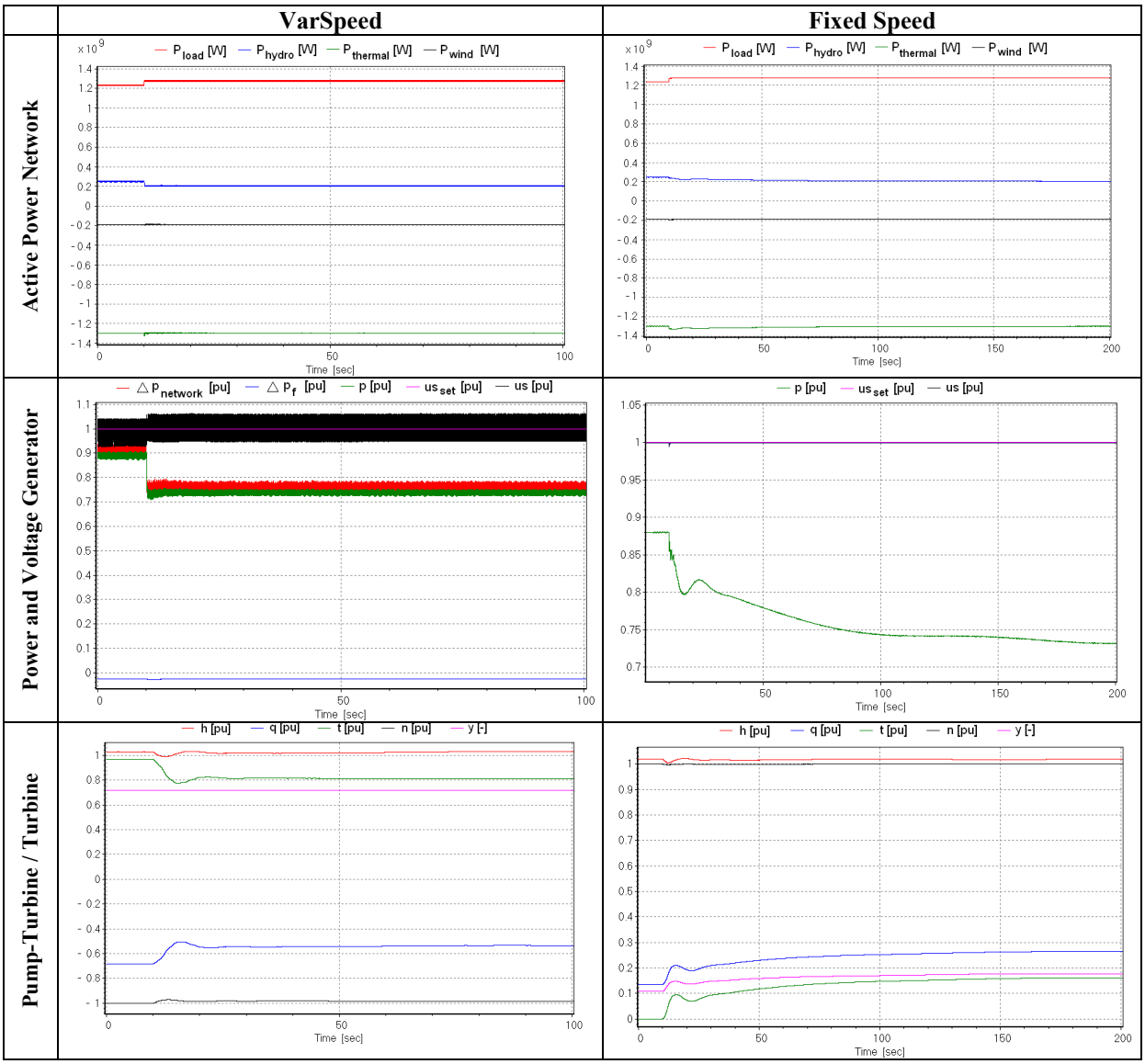

Figure 15 Comparison of the simulation results for both variable and fixed speed solutions for load acceptance in pump mode operation.

In the case of variable speed solution, the 40MW consumer load increase is almost instantaneously compensated by a reduction of the pump input power. This input power reduction is again enabled by fast reaction of the DFIG machine and by the flywheel effect. In this case, the power network requires additional power which is

provided by first kinetic energy stored in the rotating inertias leading to speed reduction and then by pump rotational speed adjustment.

The fixed speed machine is operated with hydraulic short circuit where the pump is experiencing almost steady-state operation, see Figure 16, while the load acceptance is compensated by the turbine input power adjustment. Initially the output power of the turbine is zero and is then increased to 40MW by increasing the guide vane opening through the turbine speed governor action. In this case, again the first reaction to compensate the load acceptance is given by the thermal power plant while the final power compensation is achieved by the hydropower plant.

The comparison of the resulting power network frequency and consumer load voltage is presented for the two solutions in Figure 17. The frequency deviation obtained with the variable speed machine is again about 10 times smaller than the frequency deviation obtained with the fixed speed machine. However, the comparison of the voltage of the consumer load shows a larger deviation in the case of the Varspeed than for the fixed speed solution. One may also notice that for both solutions, the head variations induced by the hydraulic machine transients are very small.

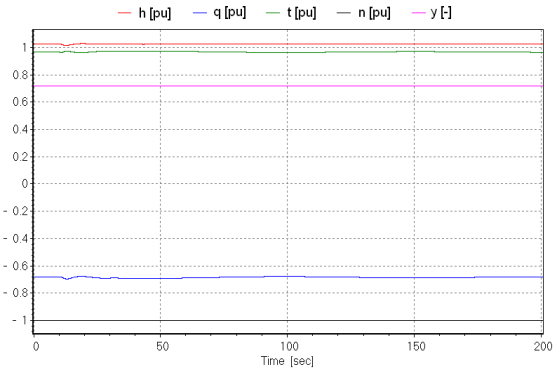

Figure 16 Transient behaviour of the pump of the fixed speed solution for load acceptance in pump mode operation.

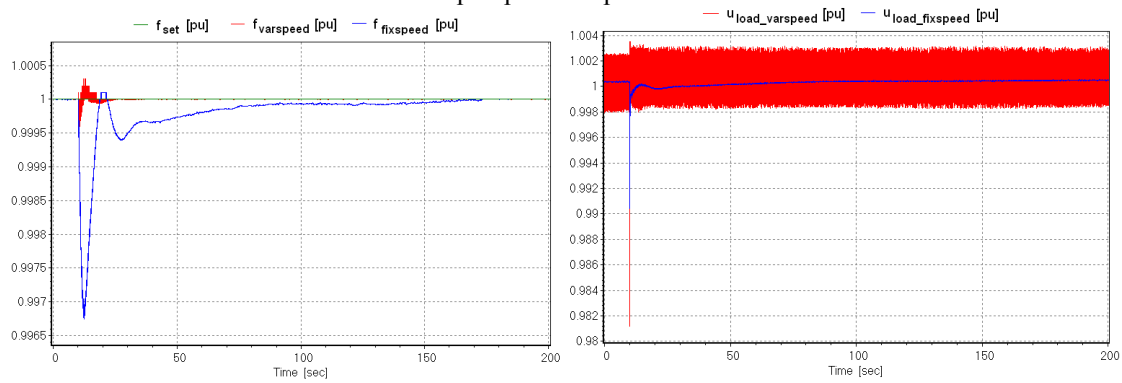

Figure 17 Comparison of the simulation results of the power network frequency (left) and voltage of the load (right) for both variable and fixed speed solutions for load acceptance in pump mode operation.

7.3. Fluctuating Wind Power Compensation in Pump Mode of Operation

The third case study consists of a wind power output variation resulting from wind velocity decrease from 22m/s to 11m/s in about 60s. The initial conditions of the power flow of the islanded power network are identical to the previous case study and are summarized in Table 6. Figure 18 presents the transient behavior of the wind farm resulting from wind decrease. During the first 40s, the wind velocity decrease has no influence on the wind farm power output as the wind turbine velocity is above the rated wind of 13m/s and the wind turbine is operated in stall control by adjusting the blade pitch angle to satisfy the maximum generator power output. Then, the power decreases of about 25% and results in power output reduction of about 50MW.

Table 6 Initial power flow before the wind increase.

Element	Active power P [MW]	Power flow
Hydropower Plant	+249.1	Consumption
Thermal Power Plant	-1297.2	Production
Wind Farm	-189.2	Production
Consumer Load	+1232.4	Consumption

Figure 19 shows the simulation results of the transient behavior of both the Varspeed and fixed speed solutions resulting from the wind velocity decrease. The transient behavior of the pump of the fixed speed solution is presented in Figure 20.

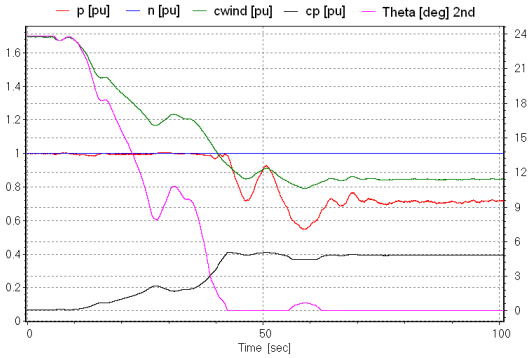

Figure 18 Transient behaviour of the wind farm resulting from wind fluctuation.

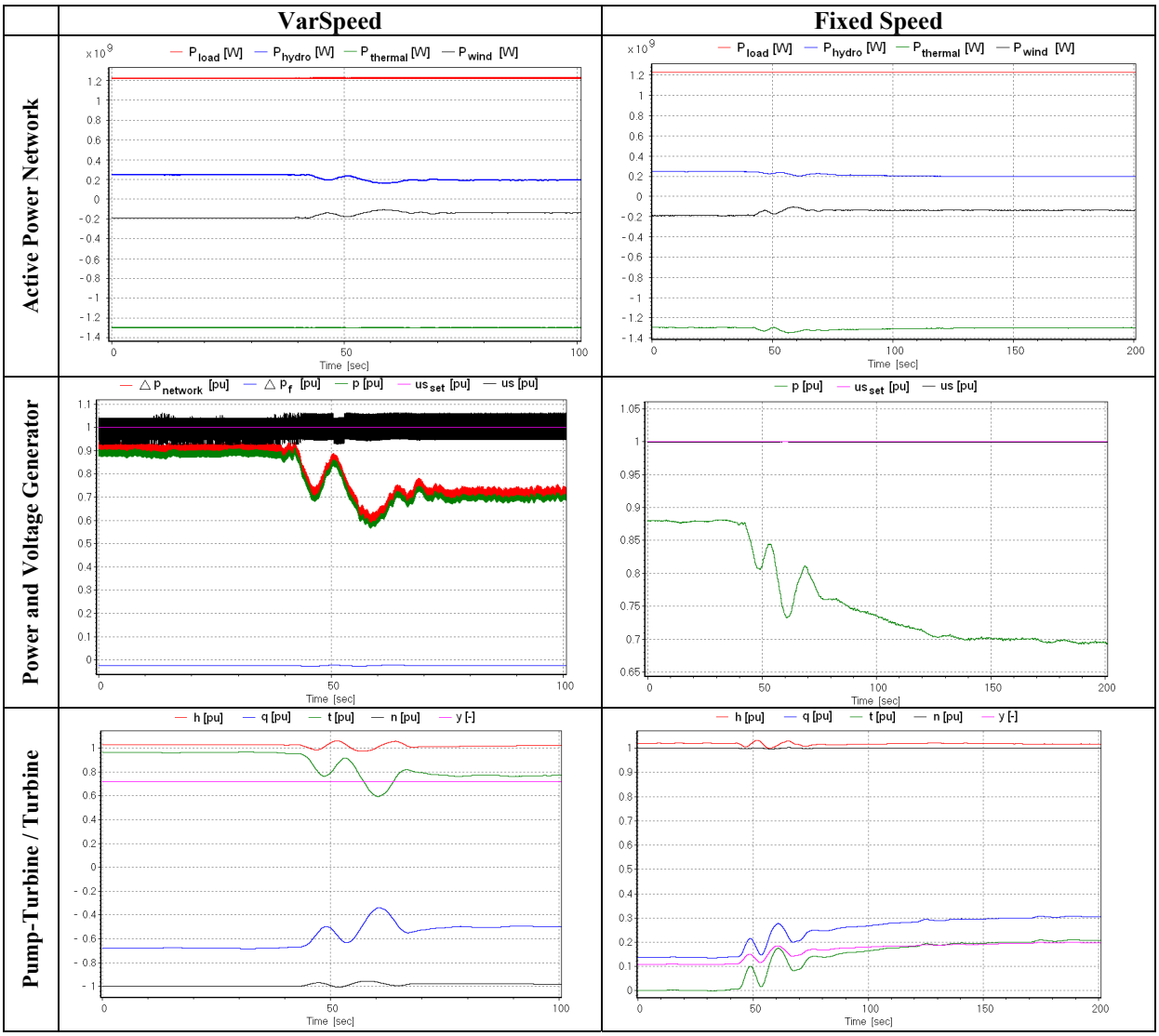

Figure 19 Comparison of the simulation results for both variable and fixed speed solutions for wind fluctuation in pump mode operation.

The variable speed unit follows very well the wind farm power output decrease through both flywheel effect and adaption of the rotational speed of the pump. For the fixed speed unit, the power input reduction is again achieved through turbine power input increase while the pump is at constant operating point. The comparison of the network frequency and load voltage obtained for the two different solutions are presented in Figure 21.

The fast response of the variable speed unit leads to frequency deviations about 20 times smaller than for the fixed speed machine. However, except the harmonics generated by the Varspeed solution, the general behavior of the voltage is rather similar for both solutions.

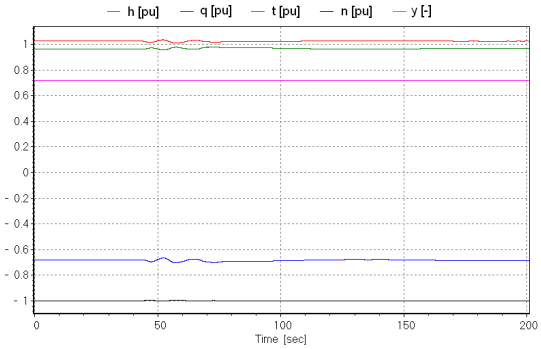

Figure 20 Transient behaviour of the pump of the fixed speed solution for wind fluctuation.

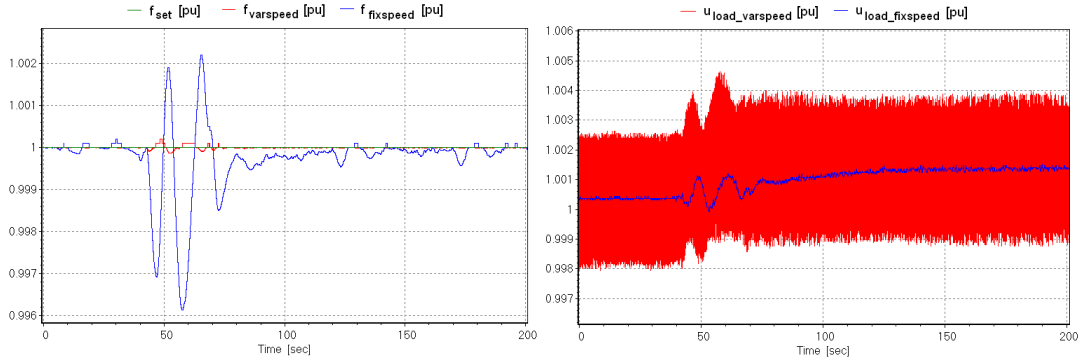

Figure 21 Comparison of the simulation results of the power network frequency (left) and voltage of the load (right) for both variable and fixed speed solutions for wind fluctuations.

8. Conclusions

This paper presents the modeling with a high level of complexity for all the energy sources including control systems of a mixed islanded power network comprising hydraulic, thermal and wind power plants and a consumer load. The capability of variable speed pump-turbine and 3 machine-type with fixed speed machines to improve the power network stability is compared through the simulation of power network disturbances.

Based on the simulation results obtained for load rejection in turbine mode, load acceptance in pump mode and wind power fluctuations in pump mode, it can be noticed that:

- both solutions contribute to power network stability by providing regulating power services;
- the variable speed unit is capable of very fast active power injection or absorption enabled by the flywheel effect and thus reduces by at least a factor 10 the frequency deviation compared to frequency deviation obtained with fixed speed machine;
- the contribution to voltage control of both solutions is very similar;
- the frequency converter on the rotor cascade of the variable speed machine induces harmonics on active power, stator currents and thus on line voltages;
- the use of 3 level VSI instead of 2 level VSI enables to reduce the amplitudes of harmonics.

Moreover, during feasibility studies, one has also to compare carefully global efficiency of the entire equipment which strongly depends on the site characteristics and all possible electromechanical solutions with the additional investment cost of 3 machine-type units compared to variable speed pump-turbine units.

This paper shows the ancillary benefits that pumped storage power plants can provide to stabilize power network and also the higher dynamic performances of variable speed solutions. However, if dynamic performances and related regulation services are important criteria, especially for mixed islanded power network, one should also address change-over capabilities, operation range and constraints, global efficiency and economical issues for the selection of appropriate technology for a hydropower project. Moreover, such kind of analysis based on multi-physics simulation approach is crucial to:

- determine and validate the appropriate technology
- define governors parameters;
- determine pump/turbine operation procedures;
- assess the power network stability;
- check the safety of the installations.

9. Acknowledgements

The authors would like to thank Dr. Jean-Jacques Hérou from EDF-CIH, and Mr. Bob Greiveldinger and Mr. Yves Vaillant both former LMH Master students, for their great contribution to the modelling of the thermal and wind farm power plants. For this paper, the authors took advantages of the development of the SIMSEN hydraulic extension, developed with the financial support of: CTI, Swiss Federal Commission for Technology and Innovation, contract awards No 5750.1 EBS, EOS, BKW FMB Energie AG, SIG, SIL, Groupe E, Electricité Suisse and PSEL Funds for Projects and Studies of the Swiss Electric Utilities, contract awards No 215 Scapin. The authors also would like to thank EDF-CIH, VOITH-Siemens Hydro Power Generation and ALSTOM Power Hydro (CTI project 8330) for their financial support and their scientific contribution in the development of the hydraulic extension of SIMSEN.

10. Nomenclature

A: pipe cross section [m^2]
A_g: gallery cross section [m^2]
A_{ST}: surge tank cross section [m^2]
D_{ref}: machine reference diameter [m]
H: net head [m]
Q: discharge [m^3/s]
N: rotational speed [rpm]
P: power [W]
T: Torque [Nm]
a: pipe wave speed [m/s]
h: piezometric head $h=z+p/(\rho g)$ [m]
g: gravity [m/s^2]
p: static pressure [Pa]
l_g: length of the gallery [m]
p: pressure [Pa]
t: time [s]
x: position [m]
y: turbine guide vane opening [-]
Z: elevation above a datum [m]
ν: specific speed $\nu = \omega_R (Q_R / \pi)^{1/2} / (2 \cdot g \cdot H_R)^{3/4}$ [-]
ω: rotational pulsation [rd/s]
$_R$: subscript for rated

References

[1] **Akhmatov, V., Knudsen, H,** "An aggregate model of a grid-connected, large-scale, offshore wind farm for power stability investigations-importance of windmill mechanical system", Electrical power and Energy Systems 24, 2002.

[2] **Bénéteau P., Esnault F.,** "Hydrodynamique transmission de puissance cours et applications", Sciences Industrielles, ELLIPSES, 1997.

[3] **Bölcs, A.,** "Turbomachines thermiques", Vol. I, LTT/EPFL, 1993.

[4] **Bucher, R.,** "Enhanced energy balancing and grid stabilisation through 3-machine-type variable-speed pumped-storage units", Proc. Int. Conf. Hydro 2007, Granada, Spain, October 2007.

[5] **Canay, I. M.,** "Extended synchronous machine model for calculation of transient processes and stability", Electric machines and Electromechanics, vol. 1, pp. 137-150, 1977.

[6] **Godfrey, K.,** "Design and application of multifrequency signals", Computing & Control Engineering Journal, Vol. 2, Issue 4, July 1991, pp.187–195.

[7] **Grotenburg, K., Koch, F., Erlich, I., Bachmann, U.,** "Modeling and Dynamic Simulation of Variable Speed Pump Storage Unit Incorporated into the German Electric Power System", EPE 2001, Graz, Austria, 2001.

[8] **Heier, S.,** "Grid integration of wind energy conversion systems", Chichester : Wiley, 1998.

[9] **Hodder, A.,** "Double-fed asynchronous motor-generator equipped with a 3-level VSI cascade", Thesis EPFL n° 2939, Switzerland, Lausanne (http://library.epfl.ch/theses/?nr=2939), 2004.

[10] **Jaeger, R. C.**, "Fluid transients in hydro-electric engineering practice ".Glasgow: Blackie, 1977.

[11] **Kopf, E., Brausewetter, S., Giese, M., Moser, F.,** "Optimized control strategies for variable speed machines," In Proceeding of the 22nd IAHR Symposium on Hydraulic Machinery and Systems, Stockholm, Sweden, June –July 2004.

[12] **Kuwabara, T., Shibuya, A., Furuta, H., Kita, E., Mitsuhashi, K.,** "Design and Dynamic Response Characteristics of 400 MW Adjustable Speed Pumped Storage Unit for Ohkawachi Power Station", IEEE Transactions on Energy Conversion, vol. 11, issue 2, pp. 376-384, June 1996.

[13] **Nicolet, C.,** "Hydroacoustic modelling and numerical simulation of unsteady operation of hydroelectric systems", Thesis EPFL n° 3751, 2007, (http://library.epfl.ch/theses/?nr=3751).

[14] **Nicolet, C., Greiveldinger, B., Hérou, J.-J., Kawkabani, B., Allenbach, P., Simond, J.-J., Avellan, F.,** "High Order Modeling of Hydraulic Power Plant in Islanded Power Network", IEEE Transactions on Power Systems, Vol. 22, Number 4, November 2007, pp.: 1870-1881.

[15] **Nicolet, C., Vaillant, Y., Kawkabani, B., Allenbach, P., Simond, J.-J., Avellan, F.,** "Pumped Storage Units to Stabilize Mixed Islanded Power Network: a Transient Analysis", Proceedings of HYDRO 2008, October 6-9, 2008, in Ljubljana, Slovenia, Paper 16.1.

[16] **Pannatier, Y., Nicolet, C., Kawkabani, B., Simond, J.-J., Allenbach, Ph.,** "Dynamic Behavior of a 2 Variable Speed Pump-Turbine Power Plant", ICEM 2008, XVIII International Conference on Electrical Machines, Vilamoura, Portugal, September 2008.

[17] **Paynter, H. M.,** "Surge and water hammer problems". Transaction of ASCE, vol. 146, p 962-1009, 1953.

[18] **Sapin, A.,** "Logiciel modulaire pour la simulation et l'étude des systèmes d'entraînement et des réseaux électriques", Thesis EPFL n° 1346, 1995, (http://library.epfl.ch/theses/?nr=1346).

[19] **Schwery, A., Fass, E., Henry, J.-M., Bach, W., Mirzaian, A.,** "Pump storage power plants, ALSTOM's long experience and technological innovation", Hydro 2005, Villach, Austria, 2005.

[20] **Simond, J.-J., Sapin, A., Schafer, D.,** "Expected benefits of adjustable speed pumped storage in the European network", Hydropower into thenext century, pp. 579-585, Gmunden, Austria , 1999.

[21] **Slootweg, J. G. , De Haan, S. W. H., Polinder, H., Kling, W. L.,** "General model for representing variable speed wind turbines in power system dynamics simulations", IEEE Transactions On Power Systems, Vol. 18, No. 1, February 2003.

[22] **Slootweg J.G., Polinder H., Kling W.L.,** "Representing wind turbines electrical generating systems in fundamental frequency simulations", IEEE Transactions on energy conversion, VOL. 18, NO. 4, 2003

[23] **Souza, O.H., Jr.; Barbieri, N.; Santos, A.H.M.;** "Study of hydraulic transients in hydropower plants through simulation of nonlinear model of penstock and hydraulic turbine model," IEEE Transactions on Power Systems, vol. 14, issue 4, pp. 1269 – 1272, 1999.

[24] **Suul, J. A., Uhlen, K., Undeland, T.,** "Variable speed pumped storage hydropopwer for integration of wind energy in isolated grids", IEEE, NORPIE/2008, Nordic Workshop on Power and Industrial Electronics, June 9-11, 2008.

[25] **Wiik, J., Gjerde, J. O., Gjengedal, T.,** "Impacts from Large Scale Integration of Wind Farms into Weak Power Systems, IEEE 2000.

[26] **Wylie, E. B. & Streeter, V.L.,** "Fluid transients in systems". Prentice Hall, Englewood Cliffs, N.J, 1993.

The Authors

Christophe NICOLET graduated from the Ecole polytechnique fédérale de Lausanne, EPFL, in Switzerland, and received his Master degree in Mechanical Engineering in 2001. He obtained his PhD in 2007 from the same institution in the Laboratory for Hydraulic Machines. Since, he is managing director and principal consultant of Power Vision Engineering Sàrl in Ecublens, Switzerland. He is also lecturer at EPFL in the field of "Flow Transients in systems".

Yves PANNATIER graduated from the EPFL and received his Master degree in Electrical Engineering in 2007. He is now PhD Student at the Laboratory for Electrical Machines of the EPFL. His main field of interest is the simulation of variable speed units in transient operation.

Basile KAWKABANI received his master degree in 1978 from SUPELEC, Ecole Supérieure d'Electricité in Paris France, and his Ph.D. degree in 1984 from the Swiss Federal Institute of Technology in Lausanne Switzerland. Since 1990, he is lecturer and senior researcher at the EPFL Laboratory for Electrical Machines. His interests include modelling of power systems, power system stability and control.

Alexander SCHWERY holds a Phd degree in Electrical Engineering from the Swiss Federal Institute of Technology (EPFL 1999) in Lausanne. He joined ALSTOM (Switzerland) Ltd in 1999 where his main fields of

application are the use and development of different simulation and calculation tools for salient pole generators. He is currently head of the electrical group in the Hydro Generator Technology Center.

Prof. François AVELLAN graduated in Hydraulic Engineering from INPG, Ecole Nationale Supérieure d'Hydraulique, Grenoble France, in 1977 and, in 1980, got his doctoral degree in engineering from University of Aix-Marseille II, France. Research associate at EPFL in 1980, he is director of the Laboratory for Hydraulic Machines since 1994 and was appointed Ordinary Professor in 2003. Prof. F. Avellan is the Chairman of the IAHR Section on Hydraulic Machinery and Systems.

Prof. Jean-Jacques SIMOND graduated in Electrical Engineering in 1967 and got his doctoral degree in 1976 from EPFL, the Swiss Federal Institute of Technology in Lausanne. Till 1990 he was working for BBC / ABB first as R&D engineer and later as head of the technical department for Hydro- and Diesel-generators. He is Professor and director of the Laboratory of Electrical Machines of the EPFL since 1990. He is also consultant for international electrical machines manufacturers and utilities.

APPENDIX 1: Comparison between 2 and 3 level Voltage Source Inverter (VSI) cascade.

A sample of time history and related amplitude spectra of steady-state stator currents generated by 2 and 3 level VSI DFIG machines connected to an infinite network are respectively presented in Figure 22 and in Figure 23. The comparison of these 2 figures shows that 3 level VSI features lower level of harmonics with a Total Harmonics Distortion THD Level reduced by factor 2.7 from 0.563% to 0.208%.

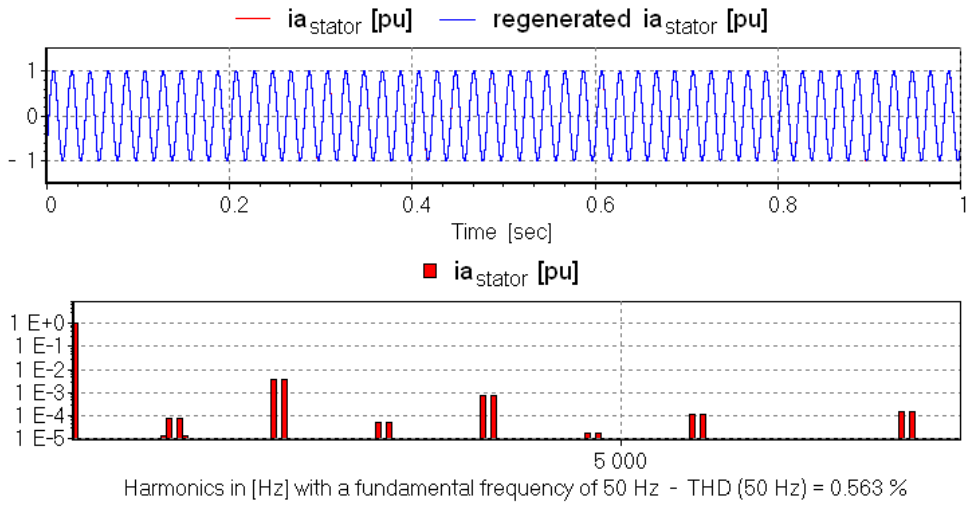

Figure 22 Stator current as function of time (top) and related amplitude spectra (bottom) obtained with 2 level VSI.

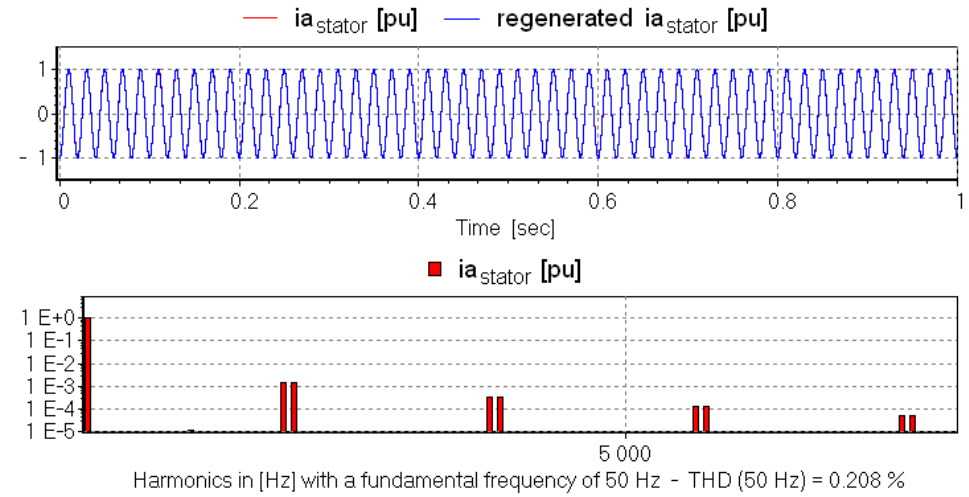

Figure 23 Stator current as function of time (top) and related amplitude spectra (bottom) obtained with 3 level VSI.

APPENDIX 2: Modeling of Hyraulic components.

Table 7 Modeling of hydraulic components with related equivalent schemes.

Component	Hydraulic scheme	Electrical equivalent scheme	Parameters
Generalized pipe	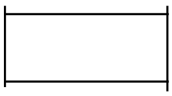	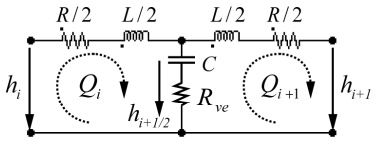	$R=\frac{dx\lambda\lvert Q\rvert}{2gDA^2}$ $R_{ve}=\frac{\mu}{\rho gAdx}$ $L=\frac{dx}{gA}$ $C=\frac{dxgA}{a^2}$
Valve	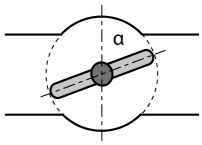	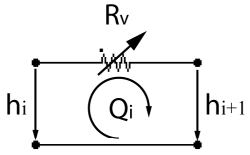	$R_v=\frac{K_v(\alpha)\lvert Q\rvert}{2gA^2}$
Surge tank	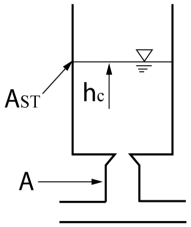	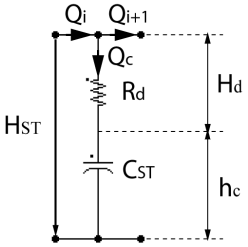	$R_d=\frac{K_d(Q)\lvert Q\rvert}{2gA^2}$ $C_{ST}=A_{ST}(h_c)$
Air vessel	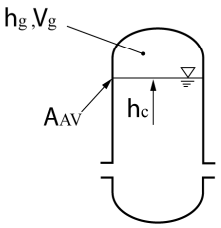	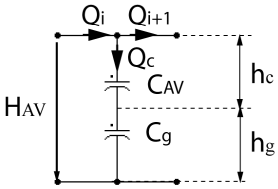	$C_{AV}=A_{AV}(h_c)$ $C_g=\frac{V_g}{h_g n}$
Cavitation	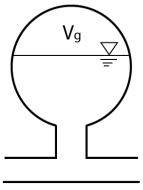	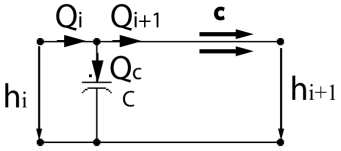	$C=\frac{\partial V_g}{\partial h_{i+1}}$ $\chi=\frac{\partial V_g}{\partial Q_{i+1}}$ $Q_c=C\cdot\frac{dh_{i+1}}{dt}+\chi\cdot\frac{dQ_{i+1}}{dt}$
Francis pump-turbine	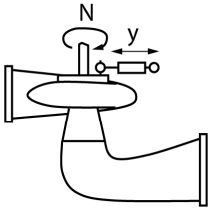	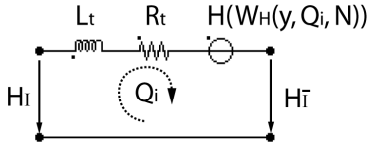	$H=H(W_H(y,Q,N))$ $T=T(W_B(y,Q,N))$ $R_t=R_t(W_H(y,Q,N))$ $L_t=\frac{l_{equ}}{gA}$

V_g : volume of gas [m³] W_H : turbine head characteristic [-] l_{equ} : turbine equivalent length [m]

h_g : pressure of gas [m] W_B : turbine torque characteristic [-] μ : viscosity of the fluid or material [Pa·s]